



HAL
open science

Microplastics and microfibers in urban runoff from a suburban catchment of Greater Paris

Robin Treilles, Johnny Gasperi, Anaïs Gallard, Mohamed Saad, Rachid Dris, Chandirane Partibane, Jérôme Breton, Bruno Tassin

► **To cite this version:**

Robin Treilles, Johnny Gasperi, Anaïs Gallard, Mohamed Saad, Rachid Dris, et al.. Microplastics and microfibers in urban runoff from a suburban catchment of Greater Paris. *Environmental Pollution*, 2021, 25 p. 10.1016/j.envpol.2021.117352 . hal-03226728

HAL Id: hal-03226728

<https://enpc.hal.science/hal-03226728>

Submitted on 26 May 2021

HAL is a multi-disciplinary open access archive for the deposit and dissemination of scientific research documents, whether they are published or not. The documents may come from teaching and research institutions in France or abroad, or from public or private research centers.

L'archive ouverte pluridisciplinaire **HAL**, est destinée au dépôt et à la diffusion de documents scientifiques de niveau recherche, publiés ou non, émanant des établissements d'enseignement et de recherche français ou étrangers, des laboratoires publics ou privés.

1 **Microplastics and microfibers in urban runoff from a suburban catchment of Greater**
2 **Paris**

3

4 Robin TREILLES ^{a*}, Johnny GASPERI ^b, Anaïs GALLARD ^a, Mohamed SAAD ^a,
5 Rachid DRIS ^a, Chandirane PARTIBANE ^a, Jérôme BRETON ^c, Bruno TASSIN ^a

6

7 ^aLeesu, Ecole des Ponts, Univ Paris Est Creteil, Marne-la-Vallee, France

8

9 ^bGERS-LEE Université Gustave Eiffel, IFSTTAR, F-44344 Bouguenais, France

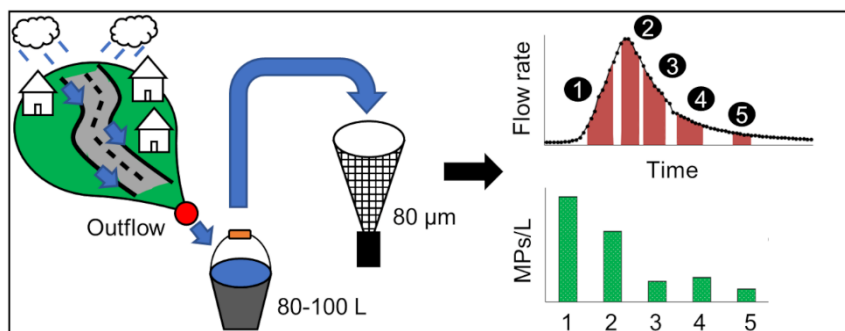
10

11 ^cDirection des Services de l'Environnement et de l'Assainissement du Val-de-Marne
12 (DSEA), Conseil départemental du Val-de-Marne, Créteil, France

13

14 *Corresponding author: robin.treilles@enpc.fr

15 **Graphical abstract**



16

17 **Abstract**

18 Microplastics (MPs) and microfibers (MFs) in stormwater have been poorly investigated. Data
19 on their concentration variation during rain events over space and time are still sparse. For
20 the first time, the variability of microliter concentrations in stormwater has been studied. MF

21 and MP concentrations were investigated in stormwater runoff at the outlet of the suburban
22 catchment at Sucy-en-Brie (a suburb of Paris, France), during four rain events with different
23 precipitation levels (2.6–8.6 mm/h). For each rain event, 3–5 samples of 80–100 L of
24 stormwater were collected and filtered through a net with an 80 µm mesh. Samples were
25 digested using sodium dodecyl sulphate and 30% H₂O₂ followed by NaI density separation.
26 The MFs were then counted using a stereomicroscope. MPs were identified using Fourier
27 transform infrared spectroscopy coupled with microscopy (µFTIR). Median MF and MP
28 concentrations were 1.9 and 29 items/L, with an interquartile range of 2.3 and 36 items/L,
29 respectively (N=18). A different pattern was observed between MFs and MPs. While no
30 relationship or trends were observed for MFs, the highest MP concentrations were observed
31 before the flow rate peak of the rain events. This could indicate a difference in the behaviour
32 between MFs and MPs. We estimated the median MP mass concentration to be 56 µg/L with
33 an interquartile range of 194 µg/L, whereas the mass concentration of macroplastics was
34 estimated to be 31 µg/L with an interquartile range of 22 µg/L at the same sampling site, in a
35 previous study. For this sampling site, MPs and macroplastics have the same order of
36 magnitude. This study may have strong implications on microplastic study in urban waters.

37 **Capsule (no more than two lines)**

38 Microfiber (MF) and microplastic (MP) median concentrations in stormwater were 1.9 and 29
39 items/L. The MP and macroplastics were in the same range of mass concentration.

40 **KEYWORDS:** Microplastic, Microfiber, Stormwater runoff, Urban effluent

41 **1. Introduction**

42 Microplastic (MP) pollution in urban hydrosystems is an emerging concern. MPs, mostly in the
43 form of microfibers (MFs), have been reported in all types of urban water: (i) the atmosphere
44 and rainwater (Dris, 2016), (ii) in drinking water (Pivokonsky et al., 2018), (iii) wastewater
45 entering wastewater treatment plants, in effluent (Talvitie et al., 2015), sludge (Mintenig et al.,
46 2017) and, (iv) more recently, in stormwater (Dris et al., 2018). However, this last type is the

47 least documented. Stormwater peak flows may reach high values depending on
 48 hydrometeorological conditions; therefore, as Hitchcock (2020) recently suggested,
 49 stormwater can play a significant role in the MP budget at the urban scale. A mini review of
 50 studies on stormwater is presented in Table 1. In those studies, MP concentrations ranged
 51 between 0.5 to 1,050 MPs/L.

52 Table 1: Microplastic concentrations in stormwater in urban drainage systems

References	Study site	Size detection limit	MPs.L ⁻¹ (min–max)	Sampling volumes (L)
Dris et al., 2018	France	80 µm	24-60 fibers.L ⁻¹ and <2-16 fragments.L ⁻¹	0.2-1.5
Eisentraut et al., 2018	Germany	10 µm	Mass estimations of polymers and SBR*	3
Liu et al.2019	Denmark	10 µm	0.49–22.9	201-454
Olesen et al., 2019a	Denmark	10 µm	270 (on average)	10
Piñon-Colin et al., 2020	Mexico	200 µm	88–275	3
Järilskog et al., 2020	Sweden	20 µm	1–100	2.7-9
Mak et al., 2020	Hong-Kong	54 µm	0.5–10	8
Bondelind et al., 2020	Sweden	20 µm	29.3–1050	Mathematical modeling

53 *SBR: *styrene butadiene rubber*

54 To the best of our knowledge, Dris et al. (2018) was the first to report the presence of MPs in
 55 stormwater using visual identification. In their results, the fibers corresponded to the most
 56 significant shape found in these samples; the MP fragments were less numerous. Eisentraut
 57 et al. (2018) used thermal extraction desorption gas chromatography mass spectrometry to
 58 identify the nature of the particles, particularly those from tire wear, in stormwater samples
 59 using chemical markers to identify styrene butadiene rubber (SBR), which corresponds to one
 60 of the main tire components. Several studies produced new data regarding the accumulation
 61 of MP fragments, fibers, and SBR particles in stormwater retention ponds and demonstrated
 62 that there were significant differences in the concentrations thereof between sampling sites
 63 (Liu et al., 2019; Olesen et al., 2019); for example, sediments in stormwater retention ponds
 64 act as MP sinks (Olesen et al., 2019).Piñon-Colin et al. (2020) provided the first data on MPs
 65 in stormwater from a semi-arid region, and found concentrations similar to those from previous
 66 studies. Other recent studies focusing on tire and bitumen wear particles showed a significant

67 concentration of these particles in stormwater (Järlskog et al., 2020). Some recent studies
68 also modelled the dispersion of traffic-related MPs from stormwater to a receiving river
69 (Bondelind et al., 2020) and showed that a significant part of the tire-related particles settled
70 in the river. As this mini-review shows, research on MFs and MPs in stormwater and urban
71 areas is still sparse. Storm events represent key moments for MP transport and contamination
72 (Hitchcock, 2020). However, although storm events are characterised by variability, there is
73 almost no data on the range and variability of MP concentrations during such events.

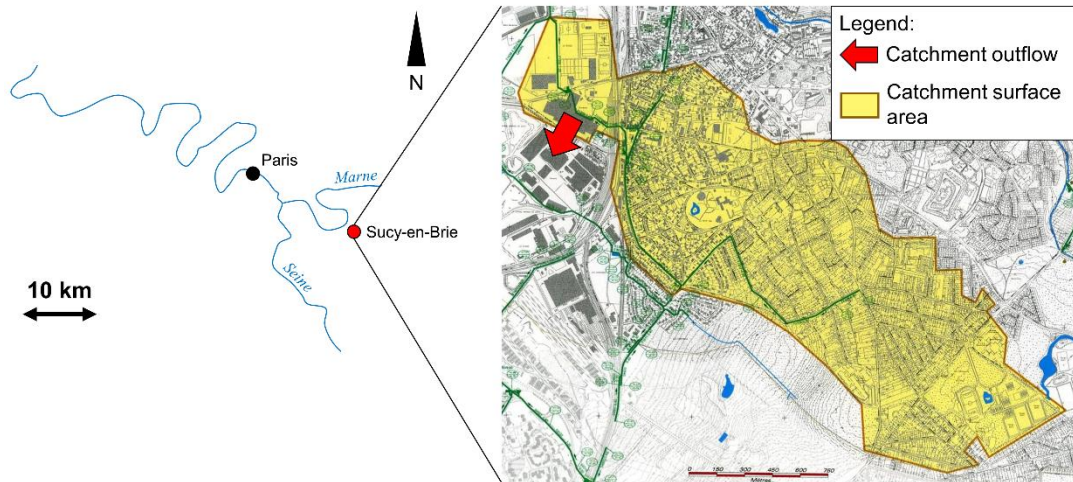
74 In this paper, we provide the concentrations of MFs and MPs for four rain events at the scale
75 of a suburban catchment in Greater Paris. We also examine the concentrations of MFs and
76 MPs during rain events as a function of rainfall intensity and flow rate. Previous works have
77 shown that the presence of non-synthetic fibers, such as the artificial and cellulose-based
78 viscose and natural fibers such as cotton, is significant in urban environments (Zhao et al.,
79 2016). Thus, all MFs with anthropogenic origins were counted. In this paper, we use the term
80 “microlitter” for all fibers and fragments investigated. Finally, this work also compares the MP
81 inputs in stormwater with those recently estimated at a corresponding sampling site (Treilles
82 et al., 2021).

83 **2. Materials and methods**

84 **2.1. Sampling site**

85 Samples were collected at the outlet of the Sucy-en-Brie catchment, which is located in a
86 suburban area south-east of the Greater Paris region (Figure 1). It has a surface area of 228
87 ha of which 62 ha is impervious (Gasperi et al., 2017). The population of the catchment is
88 ~5,700 (density of 25 cap.ha⁻¹). The area is mostly residential, with individual households that
89 correspond to a moderately dense urban area in France (Gasperi et al., 2017). However, there
90 are limited commercial and professional activities conducted in the area. Sewer systems in
91 the catchment are separated; wastewater and stormwater are collected separately. The
92 stormwater treatment device was located at the catchment outlet. Stormwater volumes and
93 precipitation levels were measured with flowmeters (DRUCK-PTX1830 and DRUCK-

94 PTX5032) and provided by Val-de-Marne Environmental and Sanitation Services Directorate
95 (DSEA 94). Samples of MPs were taken from stormwater collected, upstream from the
96 stormwater treatment device, during rain events.



97
98 Figure 1. Location and delimitation of the Sucy-en-Brie catchment

99 2.2. Sampling method

100 Four rain events that occurred from June 2018 to May 2019 where the precipitation level was
101 between 2.6 and 8.6 mm/h were studied. In comparison, the mean daily rainfall in Paris from
102 March 2018 to March 2019 was 1.7 (data from Météo France). Rain events are defined as
103 rainfall with a depth higher than 0.2 mm during 4 h. The sampling procedure was as follows:
104 for a given rain event, 3–5 consecutive samples of stormwater were collected repeatedly at
105 the same place (at the catchment outlet), using a metal bucket and filtered through an 80 µm
106 net. The sampling depth is approximately 30 cm. According to Table 1, stormwater samples
107 are generally below 10 L. Small sampling volumes may increase the variability of the results
108 and decrease their representativity. For this reason, we decided to collect a minimum of 80 L
109 and up to 100 L of stormwater for each sample. Because an automatic sampling device was
110 complex to set up, manual sampling was preferred. The net was rinsed with stormwater as
111 part of sample recovery. The samples were then stored in glass containers in a cold room (4
112 °C). The sampling of a rain event was based on weather forecasts. For these reasons, it was
113 not always possible to cover all the rain events that occurred during the study period. The

114 June 2018 and May 2019 campaigns corresponded to summer, which is characterised by
115 relatively rare and more intense storm events, whereas the December 2018 and March 2019
116 campaigns correspond to winter, which is characterised by frequent rain events with low levels
117 of precipitation. For more details, please see the hyetographs of all rain events reported in
118 Sucy-en-Brie during one week (Figure S1) and one year (Figure S2).

119 The hydrographs for each rain event sampled are presented in supplementary data (Figure
120 S3) and the sampling times are presented in the colour band. The first rain event (June 2018)
121 was the most intense, with a maximal flow rate of $\sim 2.5 \text{ m}^3/\text{s}$. Other rain events have the same
122 approximate maximal flow rate ($\sim 0.6 \text{ m}^3/\text{s}$), but their durations differ. According to our definition
123 of a rain event, March 2019 is an unusual case as it had two peaks. The shortest rain event
124 was in May 2019 (Figure S3).

125 **2.3. Preventing contamination**

126 The following precautions were taken to mitigate the risk of contamination:

- 127 • The solutions used were preliminarily filtered on glass fiber filters (GF/D Whatman,
128 Sigma Aldrich, $2.7 \mu\text{m}$). In this paper, the water and 50% ethanol used for rinsing the
129 filters is always referred to as filtered solutions.
- 130 • All glass vessels and filters were heated at $500 \text{ }^\circ\text{C}$ for 2 h before use. When needed,
131 the vessels were rinsed with water and 50% ethanol. Plastic materials were not used
132 and only 100% cotton laboratory coats were worn.
- 133 • The samples were stored in glass bottles covered with aluminium foil. All beakers used
134 during the extraction protocols were also covered with aluminium foil.
- 135 • Sieving was carried out under a laminar flow hood.
- 136 • Procedural blanks ($N = 6$) were prepared to evaluate the contamination of the samples
137 during the different steps used to extract the MPs. These underwent the same
138 processing steps as the actual samples. Each blank had an initial volume of 1 L of

139 water that was previously filtered through a GF/D filter (2.7 μm , \varnothing 90 mm). They were
140 then resuspended and analysed as samples (see the section “Analytical procedure”).

141 **2.4. Analytical procedure**

142 Stormwater samples were first sieved using both 5 mm and 1 mm sieves. The MP samples
143 were then separated into two distinct fractions: those 1–5 mm and <1 mm in size. Despite
144 sieving, long fibers (> 5 mm) were observed in the treated samples. These fibers were included
145 in the results. The 1–5 mm fraction was carefully observed on a 1 mm sieve under a binocular
146 magnifier. Particles suspected to be MPs based on their physical characteristics (colour,
147 shape, or texture) were removed and set aside in glass petri dishes to be characterised using
148 an infrared spectrometer with attenuated total reflectance (ATR; Thermo ScientificTM iD7).

149 The <1 mm fraction underwent different treatment steps, as follows: (i) pre-treatment via
150 sodium dodecyl sulphate (SDS) digestion (3.5 g/L, 50 mL) at 40 °C, while being stirred with a
151 magnetic stirrer at 300 rotations per minute (rpm) for 24 h to denature any proteins; (ii)
152 digestion in 50 mL of 30 wt% H_2O_2 at 40 °C for 48 h, while being stirred with a magnetic stirrer
153 at 300 rpm, to oxidize organic matter (OM); (iii) filtration on a metallic filter (\varnothing 90 mm, 10 μm);
154 and (iv) resuspension and densimetric separation in a NaI solution ($\rho \geq 1.6 \text{ g.cm}^{-3}$) in a
155 separating funnel. The supernatant was then recovered for microlitter analysis by filtering it on
156 the metallic filters previously used. Digestion was conducted at temperatures ≤ 40 °C to
157 prevent thermal degradation of the MPs (Treilles et al., 2020). MFs were counted manually
158 under a stereomicroscope (Leica MZ12) coupled with image analysis software (Histolab) while
159 MPs were counted using μFTIR imaging.

160 Several criteria based on the colour and shape of the MFs were considered and then used in
161 the identification of MFs (Dris et al., 2015). The size detection limit of this method was 100
162 μm .

163 Once the MFs were counted, each metallic filter was plunged into a crystallizer with 20 mL of
164 filtered water and the particles were remobilized using an ultrasonic bath for 30 s. The filtered

165 water was then poured into a 100 mL glass bottle. This resuspension step was repeated thrice.
166 The metallic filter was then rinsed for a final time with 40 mL of filtered water.
167 The glass bottle was then covered and strongly agitated for 1 min to homogenise its contents.
168 Depending on the clogging, a certain volume (2.5–20 mL or 2.5–20 %) was filtered onto a
169 Whatman® anodisc inorganic filter membrane (porosity: 0.2 µm, Ø 25 mm with a filtration
170 surface of Ø 14 mm).

171 The last sample from May 2019 was counted and analysed differently from other samples as
172 an important quantity of suspended materials were collected therein. After treatment, a sub-
173 sample of 10% of its initial mass was filtered on a metallic filter and subjected to the same
174 analytical steps as the other samples.

175 Anodisc filters were analysed via µFTIR with a Thermo Scientific Nicolet™ iN10 infrared
176 microscope in transmission mode. The detector used was a Thermo Scientific® MCT/A cooled
177 imaging detector (with a spectral range of 4000–1200 cm⁻¹ and automatic baseline correction
178 to prevent interference with the anodisc filter).

179 Once the spectral background was defined, µFTIR analyses were processed as follows:

- 180 - Using the mapping analyzing mode with one scan, all particles of three 6x6 mm
181 infrared maps were analyzed, which correspond to 70% of the filtration surface.
- 182 - Maps acquired were corrected using an atmospheric suppression.
- 183 - Maps were analysed using the MP analysis software siMPle, which was developed at
184 Aalborg University, Denmark, and the Alfred Wegener Institute, Germany (Liu et al.,
185 2019).

186 The size detection limit of this method was 25 µm. Each spectrum was checked, after the
187 analysis was complete, to prevent errors. Particular attention was paid to PE spectra, as other
188 studies (Witzig et al., 2020) have noted false positive particle detection. The analysis software
189 siMPle allows the assessment of the number, mass, and volume of MPs; this is explained in
190 Kirstein et al.. (2021). MP concentrations were extrapolated to the initial sampling volumes.
191 As the number of samples was small, non-parametric statistics were used in the analysis of
192 the results.

193 It is worth noting that MF concentrations correspond to the anthropogenic microfibers with no
194 distinction of nature (synthetic, artificial and natural-cellulosic), as this fibers were only
195 counted. MP concentrations correspond to all synthetic particles found in our samples after
196 μ FTIR analyses. Thus, MF concentrations and MP concentrations are independent as the
197 methods used to collect these data are different.

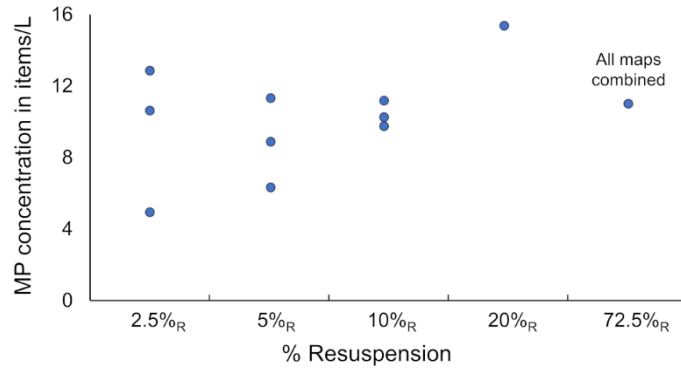
198 **3. Results**

199 **3.1. Variability of analyses using Fourier transform infrared spectroscopy** 200 **coupled with microscopy (μ FTIR)**

201 The variability of the analytical methods used for analysing MPs has not generally been
202 investigated in previous studies. Therefore, we decided to assess the variability of the μ FTIR
203 method used in this study. To do this, the same sample was resuspended several times at the
204 various resuspension percentages given below (in %_R):

- 205 - in triplicate at 2.5%_R;
- 206 - in triplicate at 5%_R;
- 207 - in triplicate at 10%_R;
- 208 - Once at 20%_R.

209 The results, which are shown in Figure 2, enabled the assessment of the variability using the
210 resuspension percentage. The variation between the first and third quartiles for 2.5%_R, 5%_R,
211 and 10%_R were 121%, 81%, and 15%, respectively. The variability decreased when the
212 resuspension percentage increased. A variation of 48% was observed between the median
213 concentration with 10 %_R and the reported concentration with 20%_R. More details are given in
214 the supplementary data (Figure S4 and Figure S5).



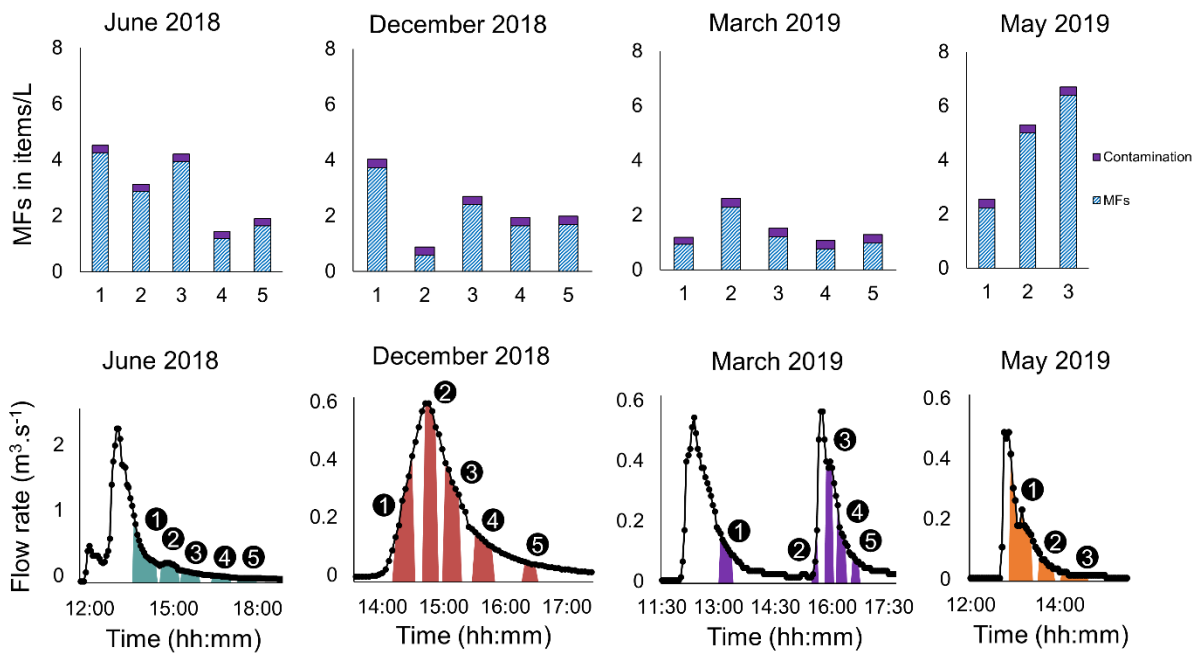
215

216 Figure 2: Microplastic (MP) concentrations estimated in items/L in different resuspension
 217 percentages (%_R) for the same stormwater sample

218 3.2. Anthropogenic microfibers in stormwater

219 Anthropogenic MF concentrations estimated via counting are shown in Figure 3. The sampling
 220 volumes and number of MFs in each sample are given in Table S1. The analytical blanks
 221 contained 26 fiber MFs with an interquartile range of 5 MFs (N = 6). The contamination is
 222 shown in Figure 3.

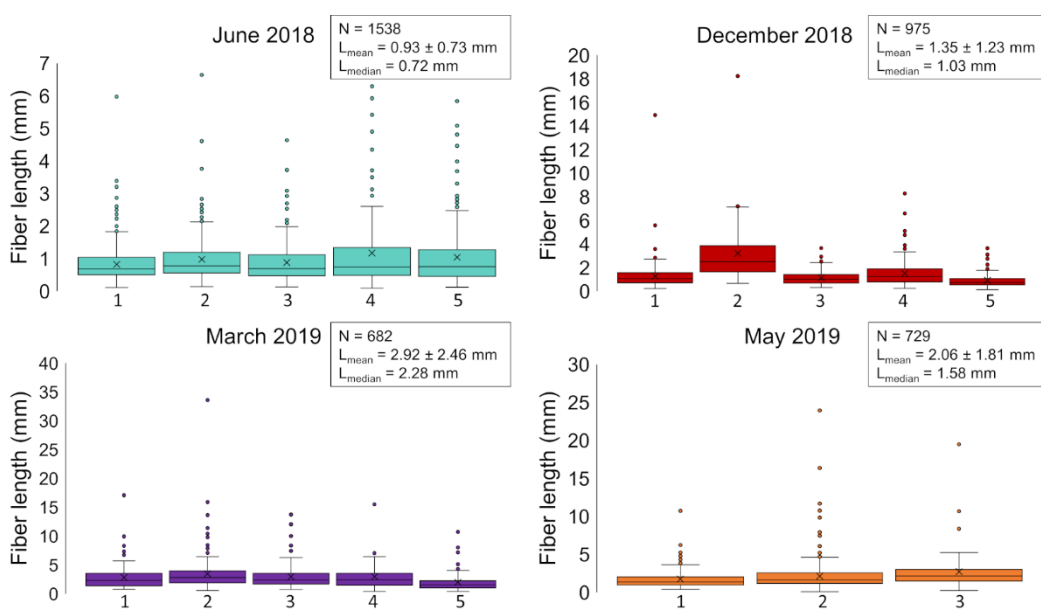
223



224

225 Figure 3. Hydrographs for each rain event studied showing microfiber (MF) concentrations in
226 items/L

227 When all samples were combined, the mean MF concentration was 2.5 ± 1.3 MFs/L (mean \pm
228 standard deviation) with a median value of 1.9 MFs/L and an interquartile range of 2.3 MFs/L
229 (N = 18). The highest concentration was observed during the last campaign (May 2019). The
230 size distribution of particles in each sample and the mean length of all MFs found in samples
231 from each rain event are shown in Figure 4.



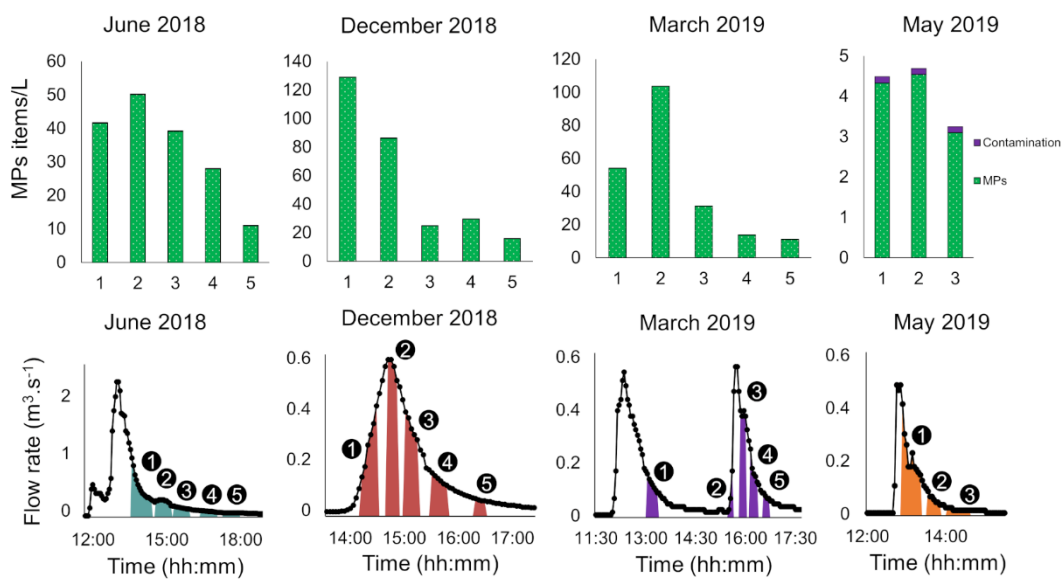
232
233 Figure 4. Size distribution of particles in each sample and each rain event; N = total number
234 of fibers found in each sampling campaign; L_{mean} = mean length of all fibers \pm standard
235 deviation, L_{median} = median length of all fibers

236 For all campaigns, the mean fiber length ranged between 0.93–2.92 mm; the median values
237 were always lower than these, ranging between 0.72–2.28 as a reflection of the significant
238 presence of fibers > 5 mm and the large number of fibers present that were <1 mm. Among
239 all the fibers counted, the maximum size found was 33.6 mm while the minimum size was 94
240 μm .

241 **3.3. Microplastics in stormwater**

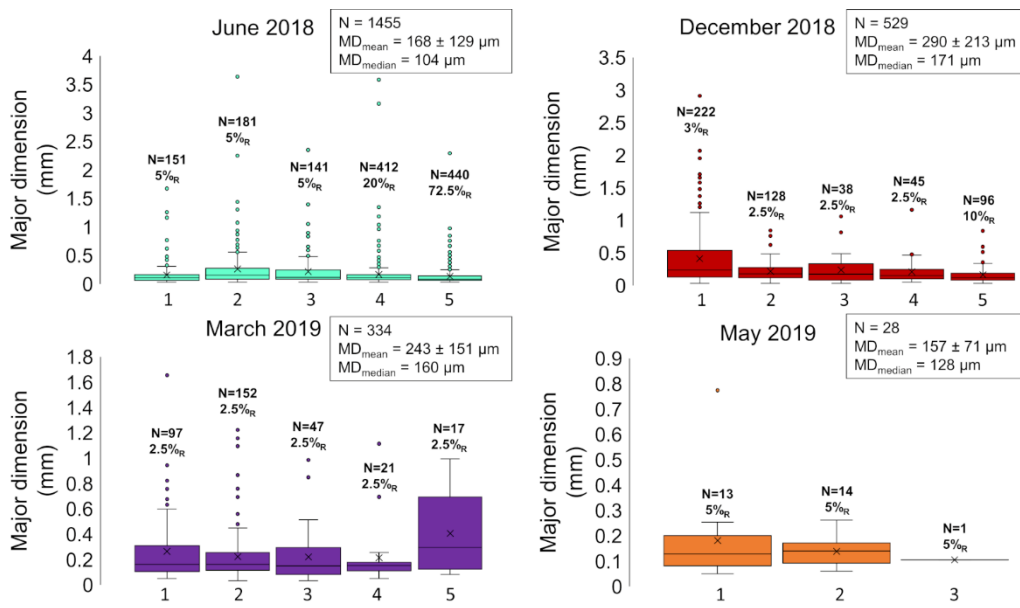
242 The analytical blanks show a variable contamination of 13 MPs with an interquartile range of
243 28 MPs (N = 6); this was negligible for almost all samples, with the exception of the last
244 campaign (May 2019) (Figure 5).

245 Figure 5 presents the concentration of MP in items/L and the hydrographs of each rain event.
246 The concentrations ranged from 3–129 items/L (min–max) with a median of 29 items/L and
247 an interquartile range of 36 items/L (N = 18).



248
249 Figure 5. Hydrographs for each rain event studied showing the concentration of microplastics
250 (MPs) in items/L

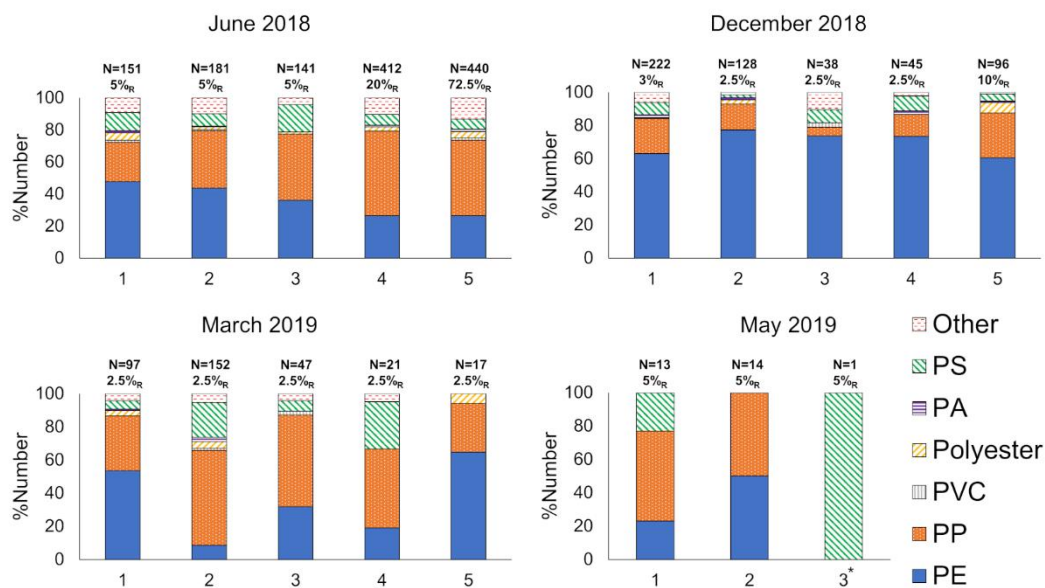
251 The major dimension (length) of all MPs identified for each sample using μ FTIR are presented
252 in Figure 6. In these boxplots, the mean values of the major dimensions are higher than
253 median values due to the sizes of the largest MPs observed. The mean particle sizes found
254 in December 2018 and March 2019 campaigns were larger than those found in the other two
255 campaigns.



256

257 Figure 6. Boxplots of the major MP dimensions found in each sample and during each
 258 sampling campaign. MD_{mean} = mean major dimension ± standard deviation;
 259 MD_{median} = median major dimension for a campaign; %_R: resuspension percentage; N:
 260 Number of MPs found for a given resuspension volume.

261 Figure 7 shows the proportion of each polymer type, with polyethylene (PE), polypropylene
 262 (PP), and polystyrene (PS) corresponding to the predominant polymers. Only a few MPs were
 263 found in May 2019, which explains the distribution observed during this campaign.



264

265 Figure 7. Percentage of polymers in each sample. N: Number of microplastics (MP) particles
 266 found for a given resuspension volume; %_R: resuspension percentage. PE: polyethylene; PP:
 267 polypropylene; PVC: polyvinyl chloride; PA: polyamide; PS: polystyrene. Only 10% of the initial
 268 mass was used in the sample marked *.

269 4. Discussion

270 4.1. Anthropogenic microfibers in stormwater

271 No correlation was found between the MF concentration and mean flow rate for each sampling
 272 period (Figure S6); the results do not even present a particular pattern depending on the latter.
 273 MF concentrations ranged between 0.6–6.4 MFs/L (min-max values) among the different
 274 samples and rain events (Figure 3). These concentrations were lower than those reported by
 275 Dris et al. 2018, who found a concentration of 24–60 fibers/L in runoff; however, Dris et al.
 276 (2018) used raw water samples that were expected to have a higher MP concentration than
 277 pre-filtered samples.

278 The median length of the particles found was > 0.72 mm for all campaigns (Figure 4). Our
 279 results suggest a significant presence of relatively long fibers in stormwater. Sutton et al.
 280 (2016) showed that 53% of the fibers sampled in urban waters from San Francisco Bay were
 281 sized 0.355–0.999 mm; this corresponds approximately to our results according to the median

282 values we obtained. Given this size distribution, the fibers we analysed do not appear to have
283 originated from atmospheric deposition, given that they are predominantly small in size at <
284 600 μm (Allen et al., 2019; Cai et al., 2017; Dris et al., 2017). The fibers found could have
285 come primarily from the wear and tear of textile products.

286 **4.2. Microplastics in stormwater**

287 We observed MP concentrations that ranged between 3–129 items/L (min–max values) with
288 a median of 29 items/L and an interquartile range of 36 items/L; these are the same order of
289 magnitude as previous studies (Järnskog et al., 2020; Olesen et al., 2019; Piñon-Colin et al.,
290 2020). A comparison between the concentrations and hydrographs in Figure 5 reveals the
291 global trends for these results. The highest concentrations were observed in December 2018
292 and March 2019. During these two campaigns, the concentration peaks could be linked to the
293 increase in flow rate. The MP concentrations just before the flow rate reached its peak were
294 six times higher than the concentration reported at the end of the rain event (Figure 5). MP
295 behaviour could be comparable to that of suspended material during flood events (Tockner et
296 al., 1999). However, the MP concentrations decreased after the peak in the flow rate. More
297 data should be collected to confirm these trends. The rain event in May 2019 was the shortest
298 and had the lowest MP concentrations. We infer that MP remobilization occurs during rain
299 events that are sufficiently intense (>2.5 mm/h and longer than 2h). For example, if MPs
300 becoming remobilized once the flow rate reaches a certain threshold could explain the low
301 concentrations found during this sampling campaign. However, this variation was not present
302 for the MFs. MFs and MPs may thus have different accumulation dynamics in environmental
303 matrices.

304 A total of 2,346 particles overall were identified as MPs. The mean major dimension for MPs
305 found in stormwater was 207 μm with a standard deviation of 273 μm ; this shows a high
306 variability. The median value was 115 μm , with 80% of the particles being less than 255 μm
307 long. This repartition shows the importance of utilising sampling devices with mesh sizes less
308 than 300 μm . Despite pre-filtration with an 80 μm mesh net, 20% of the particles were smaller

309 than 75 μm , which can be explained by clogging. A smaller mesh size may help to study
310 smaller particles. However, clogging is more frequent with smaller mesh sizes. For this reason,
311 several mesh sizes may be tested for both microplastic and microfiber samples. Large
312 particles (>1 mm) were also observed in these samples. The largest MPs were found in the
313 sample from December 2018, among the four studied rain events, whereas those from June
314 2018 and May 2019 contained the smallest MPs (Figure 6). However, these present no clear
315 trends in terms of the impact of stormwater flow rate on size of MP found.

316 In all samples, PE, PP, and PS generally made up more than 85% of the polymers found.
317 These polymers are the most common and lightest synthetic polymers. Other polymers are
318 observed occasionally.

319 The mass discharge of MPs in stormwater was estimated at 56 $\mu\text{g/L}$ with an interquartile range
320 of 194 $\mu\text{g/L}$ ($N = 18$). The interquartile range of this discharge reflects the high variability in
321 this estimation. These estimates are approximate and provide information on the order of
322 magnitude of the MP concentrations. However, when compared with the data in the literature,
323 the mass concentrations found were significant. In stormwater retention ponds in Denmark,
324 Liu et al., (2019) found a median mass concentration of 0.231 $\mu\text{g/L}$; our estimates are two
325 orders of magnitude higher than this study. That can possibly be explained by two factors. The
326 first is the quality of the stormwater, since the sampling site is in the vicinity of a densely
327 populated suburban catchment, a poor stormwater quality is expected and the second is the
328 difference in the dynamics of stormwater retention ponds (in which sedimentation can occur)
329 and stormwater runoff (which may transport more MPs).

330 Macroplastic concentration was measured at 31 $\mu\text{g/L}$ with an interquartile range of 22 $\mu\text{g/L}$
331 ($N = 15$) at the same sampling site in a previous study (Treilles et al., 2021). Macroplastics
332 are defined as plastic waste larger than 5 mm. For this sampling site, MPs mass
333 concentrations are of the same order of magnitude than macroplastics. This is unexpected but
334 can be explained by three parameters: (i) the small size of the MPs, which facilitates their
335 transport; (ii) the abundance of MPs in urban environments; and (iii) waste management

336 systems being made to reduce visible plastic and macrowaste such as macroplastics. In terms
337 of MPs, there is no method that screens these particles in stormwater, which could thus
338 contain a high concentration –in terms of numbers and mass–of MPs.

339 In the future, influence of different key factors may be considered to improve the
340 comprehension of the MF and MP transport in stormwater such as: wind trends, the
341 seasonality, the population behaviour and the degradation dynamic of macroplastics.

342 **5. Conclusion**

343 This study provides new data regarding microlitter pollution in stormwater in a suburban area.
344 The concentration of MFs in the stormwater ranged from 0.6–6.4 MFs/L, whereas that of MPs
345 ranged from 3–129 items/L. In all sampling campaigns, the median MF sizes were always >
346 0.72 mm and characterised by the presence of long fibers (those > 5 mm). These fibers are
347 most likely caused by the degradation of larger objects. The concentration of MPs varied with
348 the stormwater flow rate; higher concentrations corresponded to samples collected
349 immediately before the latter peaked. Furthermore, the behaviour of MPs may be similar to
350 the dynamics of suspended materials during rain events. In terms of their sizes, MPs in
351 stormwater had a median major dimension of 115 μm and 80% of all the MPs found were
352 smaller than 255 μm . For almost all samples, more than 85% of all the polymers found were
353 PE, PP, and PS. When compared with a previous study, the median concentrations of MP
354 were surprisingly of the same order of magnitude than those of macroplastics: the values were
355 56 $\mu\text{g/L}$ with an interquartile range 194 $\mu\text{g/L}$ for MPs and 31 $\mu\text{g/L}$ with an interquartile range
356 of 22 $\mu\text{g/L}$ for macroplastics. However, this may have been because MPs may be easily
357 transported in urban areas. Additional studies should be performed on microlitter in stormwater
358 in other urban catchments for comparison with these results as this could help form an
359 estimate of the MP mass fluxes in the environment.

360 **6. Acknowledgements**

361 We would like to thank the Urban Pollutants Observatory (OPUR) project for its support as
362 well as OSU-Efluve.

363 References

- 364 Allen, S., Allen, D., Phoenix, V.R., Le Roux, G., Durántez Jiménez, P., Simonneau, A., Binet,
365 S., Galop, D., 2019. Atmospheric transport and deposition of microplastics in a
366 remote mountain catchment. *Nat. Geosci.* 12, 339–344.
367 <https://doi.org/10.1038/s41561-019-0335-5>
- 368 Bondelind, M., Sokolova, E., Nguyen, A., Karlsson, D., Karlsson, A., Björklund, K., 2020.
369 Hydrodynamic modelling of traffic-related microplastics discharged with stormwater
370 into the Göta River in Sweden. *Environ. Sci. Pollut. Res.*
371 <https://doi.org/10.1007/s11356-020-08637-z>
- 372 Cai, L., Wang, J., Peng, J., Tan, Z., Zhan, Z., Tan, X., Chen, Q., 2017. Characteristic of
373 microplastics in the atmospheric fallout from Dongguan city, China: preliminary
374 research and first evidence. *Environ. Sci. Pollut. Res.* 24, 24928–24935.
375 <https://doi.org/10.1007/s11356-017-0116-x>
- 376 Dris, R., 2016. First assessment of sources and fate of macro and micro plastics in urban
377 hydrosystems: Case of Paris megacity 271.
- 378 Dris, R., Gasperi, J., Mirande, C., Mandin, C., Guerrouache, M., Langlois, V., Tassin, B.,
379 2017. A first overview of textile fibers, including microplastics, in indoor and outdoor
380 environments. *Environ. Pollut.* 221, 453–458.
381 <https://doi.org/10.1016/j.envpol.2016.12.013>
- 382 Dris, R., Gasperi, J., Tassin, B., 2018. Sources and Fate of Microplastics in Urban Areas: A
383 Focus on Paris Megacity. *Freshw. Microplastics* 69–83. [https://doi.org/10.1007/978-](https://doi.org/10.1007/978-3-319-61615-5_4)
384 [3-319-61615-5_4](https://doi.org/10.1007/978-3-319-61615-5_4)
- 385 Eisentraut, P., Dümichen, E., Ruhl, A.S., Jekel, M., Albrecht, M., Gehde, M., Braun, U.,
386 2018. Two Birds with One Stone—Fast and Simultaneous Analysis of Microplastics:
387 Microparticles Derived from Thermoplastics and Tire Wear. *Environ. Sci. Technol.*
388 *Lett.* 5, 608–613. <https://doi.org/10.1021/acs.estlett.8b00446>
- 389 Gasperi, J., SEBASTIAN, C., Ruban, V., DELAMAIN, M., Percot, S., Wiest, L., Mirande, C.,
390 Caupos, E., Demare, D., DIALLO KESSOO, M., Saad, M., Schwartz, J., Dubois, P.,
391 Fratta, C., WOLFF, H., Moilleron, R., Chebbo, G., Cren, C., MILLET, M., Barraud, S.,
392 Gromaire, M.-C., 2017. Contamination des eaux pluviales par les micropolluants:
393 avancées du projet INOGEV. *Tech. Sci. Méthodes* pp.51-66.
394 <https://doi.org/10.1051/tsm/201778051>
- 395 Hitchcock, J.N., 2020. Storm events as key moments of microplastic contamination in
396 aquatic ecosystems. *Sci. Total Environ.* 734, 139436.
397 <https://doi.org/10.1016/j.scitotenv.2020.139436>
- 398 Järlskog, I., Strömvall, A.-M., Magnusson, K., Gustafsson, M., Polukarova, M., Galfi, H.,
399 Aronsson, M., Andersson-Sköld, Y., 2020. Occurrence of tire and bitumen wear
400 microplastics on urban streets and in sweepsand and washwater. *Sci. Total Environ.*
401 729, 138950. <https://doi.org/10.1016/j.scitotenv.2020.138950>
- 402 Kirstein, I.V., Hensel, F., Gomiero, A., Iordachescu, L., Vianello, A., Wittgren, H.B.,
403 Vollertsen, J., 2021. Drinking plastics? – Quantification and qualification of
404 microplastics in drinking water distribution systems by μ FTIR and Py-GCMS. *Water*
405 *Res.* 188, 116519. <https://doi.org/10.1016/j.watres.2020.116519>
- 406 Liu, F., Olesen, K.B., Borregaard, A.R., Vollertsen, J., 2019. Microplastics in urban and
407 highway stormwater retention ponds. *Sci. Total Environ.* 671, 992–1000.
408 <https://doi.org/10.1016/j.scitotenv.2019.03.416>
- 409 Mak, C.W., Tsang, Y.Y., Leung, M.M.-L., Fang, J.K.-H., Chan, K.M., 2020. Microplastics
410 from effluents of sewage treatment works and stormwater discharging into the
411 Victoria Harbor, Hong Kong. *Mar. Pollut. Bull.* 157, 111181.
412 <https://doi.org/10.1016/j.marpolbul.2020.111181>
- 413 Mintenig, S.M., Int-Veen, I., Löder, M.G.J., Primpke, S., Gerdt, G., 2017. Identification of
414 microplastic in effluents of waste water treatment plants using focal plane array-
415 based micro-Fourier-transform infrared imaging. *Water Res.* 108, 365–372.
416 <https://doi.org/10.1016/j.watres.2016.11.015>

417 Olesen, K.B., Stephansen, D.A., van Alst, N., Vollertsen, J., 2019. Microplastics in a
418 Stormwater Pond. *Water* 11, 1466. <https://doi.org/10.3390/w11071466>

419 Piñon-Colin, T. de J., al., 2020. Microplastics in stormwater runoff in a semiarid region,
420 Tijuana, Mexico. *Sci. Total Environ.* 704, 135411.
421 <https://doi.org/10.1016/j.scitotenv.2019.135411>

422 Pivokonsky, M., Cermakova, L., Novotna, K., Peer, P., Cajthaml, T., Janda, V., 2018.
423 Occurrence of microplastics in raw and treated drinking water. *Sci. Total Environ.*
424 643, 1644–1651. <https://doi.org/10.1016/j.scitotenv.2018.08.102>

425 Sutton, R., Mason, S.A., Stanek, S.K., Willis-Norton, E., Wren, I.F., Box, C., 2016.
426 Microplastic contamination in the San Francisco Bay, California, USA. *Mar. Pollut.*
427 *Bull.* 109, 230–235. <https://doi.org/10.1016/j.marpolbul.2016.05.077>

428 Talvitie, J., Heinonen, M., Pääkkönen, J.-P., Vahtera, E., Mikola, A., Setälä, O., Vahala, R.,
429 2015. Do wastewater treatment plants act as a potential point source of
430 microplastics? Preliminary study in the coastal Gulf of Finland, Baltic Sea. *Water Sci.*
431 *Technol.* 72, 1495–1504. <https://doi.org/10.2166/wst.2015.360>

432 Tockner, K., Pennetzdorfer, D., Reiner, N., Schiemer, F., Ward, J.V., 1999. Hydrological
433 connectivity, and the exchange of organic matter and nutrients in a dynamic river–
434 floodplain system (Danube, Austria). *Freshw. Biol.* 41, 521–535.
435 <https://doi.org/10.1046/j.1365-2427.1999.00399.x>

436 Treilles, R., Cayla, A., Gaspéri, J., Strich, B., Ausset, P., Tassin, B., 2020. Impacts of organic
437 matter digestion protocols on synthetic, artificial and natural raw fibers. *Sci. Total*
438 *Environ.* 748, 141230. <https://doi.org/10.1016/j.scitotenv.2020.141230>

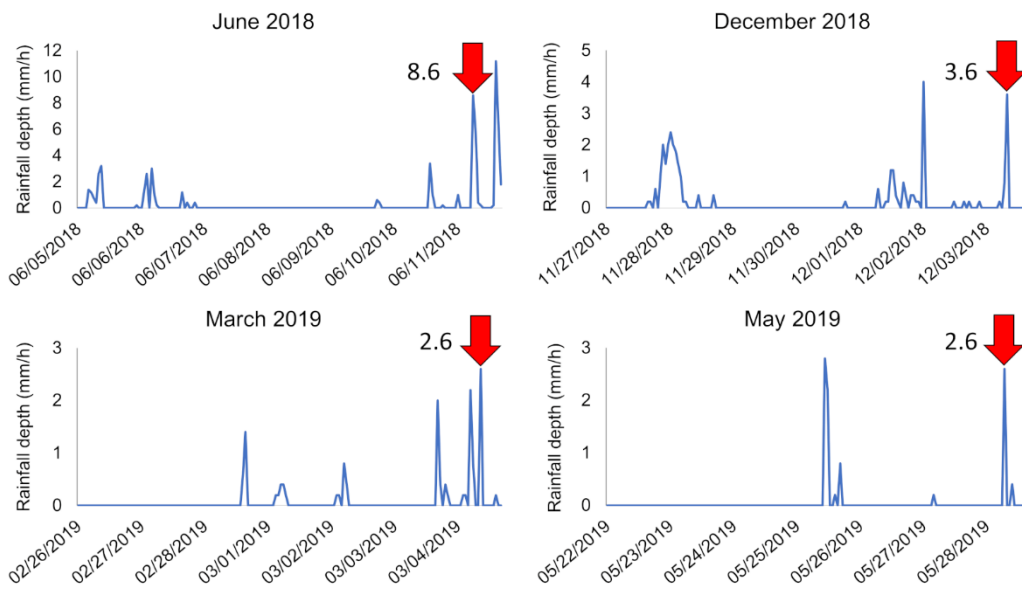
439 Treilles, R., Gasperi, J., Saad, M., Tramoy, R., Breton, J., Rabier, A., Tassin, B., 2021.
440 Abundance, composition and fluxes of plastic debris and other macrolitter in urban
441 runoff in a suburban catchment of Greater Paris. *Water Res.* 192, 116847.
442 <https://doi.org/10.1016/j.watres.2021.116847>

443 Witzig, C.S., Földi, C., Wörle, K., Habermehl, P., Pittroff, M., Müller, Y.K., Lauschke, T.,
444 Fiener, P., Dierkes, G., Freier, K.P., Zumbülte, N., 2020. When Good Intentions Go
445 Bad—False Positive Microplastic Detection Caused by Disposable Gloves. *Environ.*
446 *Sci. Technol.* 54, 12164–12172. <https://doi.org/10.1021/acs.est.0c03742>

447 Zhao, S., Zhu, L., Li, D., 2016. Microscopic anthropogenic litter in terrestrial birds from
448 Shanghai, China: Not only plastics but also natural fibers. *Sci. Total Environ.* 550,
449 1110–1115. <https://doi.org/10.1016/j.scitotenv.2016.01.112>

450

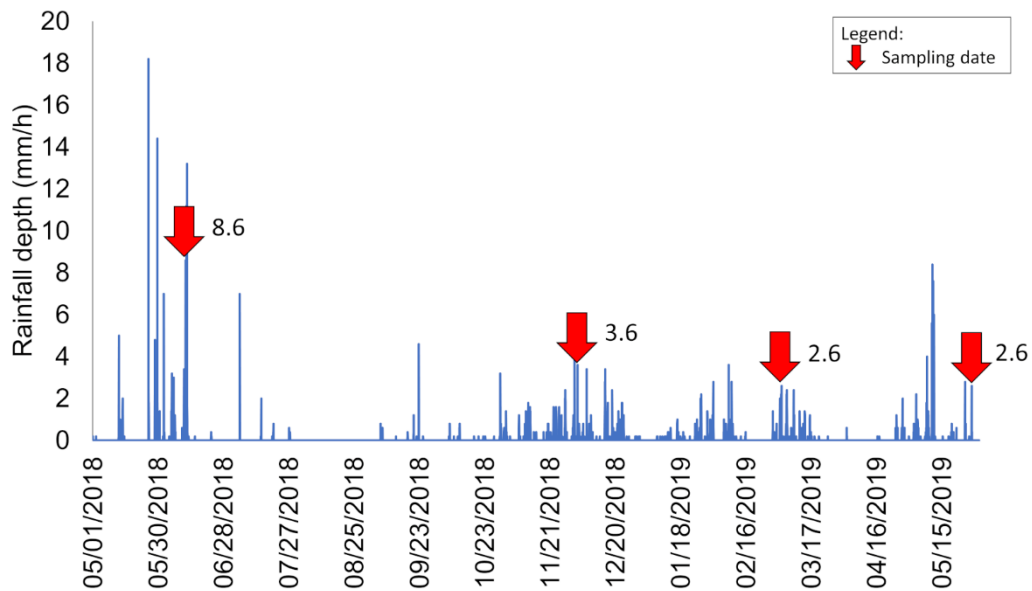
451 Supplementary data



452

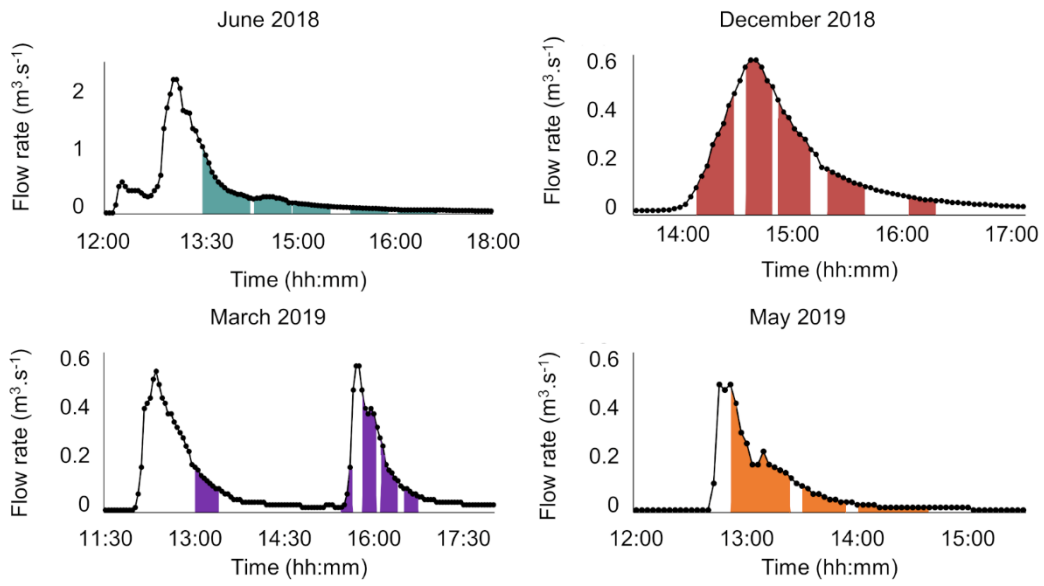
453 Figure S1: Weekly hyetographs of all rain events for each sampling campaign; the sampling
 454 dates are represented by the red arrows (data from DSEA 94 collected in Sucy-en-Brie)

455



456

457 Figure S2: Hyetograph of all rain events from March 2018 to May 2019; sampled rain events
 458 are marked with the red arrows



459

460 Figure S3: Hydrograph of each rain event sampled. Sampling periods are represented in the

461 colour bands. Note that the y-axis differs for the first event (June 2018)

462

463

	Map 1	Map 2	Map 3	All maps combined	Concentrations (items/L)
Filter 1 – 2.5 %_R	N = 9 	N = 4 	N = 6 	N = 19 	10.5
Filter 2 – 2.5 %_R	N = 8 	N = 7 	N = 8 	N = 23 	12.7
Filter 3 – 2.5 %_R	N = 0	N = 2 	N = 7 	N = 9 	4.9
Filter 1 – 5 %_R	N = 10 	N = 7 	N = 5 	N = 22 	6.1
Filter 2 – 5 %_R	N = 6 	N = 14 	N = 11 	N = 31 	8.6
Filter 3 – 5 %_R	N = 15 	N = 17 	N = 8 	N = 40 	11

■ PE ■ PP ■ PVC ■ Polyester ■ PA ■ PS ■ Other

464

465 Figure S4: Number and types of microplastics and estimated concentrations found in the
 466 sample June 2018_5 with various resuspension percentages (triplicates of 2.5%_R and 5%_R);

467 PE: polyethylene; PP: polypropylene; PVC: polyvinyl chloride; PA: polyamide; PS: polystyrene

	Map 1	Map 2	Map 3	All maps combined	Concentrations (items/L)
Filter 1 – 10 % _R	N = 28 	N = 13 	N = 31 	N = 72 	9.9
Filter 2 – 10 % _R	N = 29 	N = 9 	N = 30 	N = 68 	9.4
Filter 3 – 10 % _R	N = 25 	N = 19 	N = 34 	N = 78 	10.8
Filter 1 – 20 % _R	N = 110 	N = 61 	N = 37 	N = 208 	14.7
All filters combined 72.5 % _R				N = 570 	11.1

■ PE ■ PP ■ PVC ■ Polyester ■ PA ■ PS ■ Other

468

469 Figure S5: Number and types of microplastics and estimated concentrations found in the

470 sample June 2018_5 with various resuspension percentages (triplicates of 10%_R, one sample

471 at 20%_R and all resuspensions combined); PE: polyethylene; PP: polypropylene; PVC:

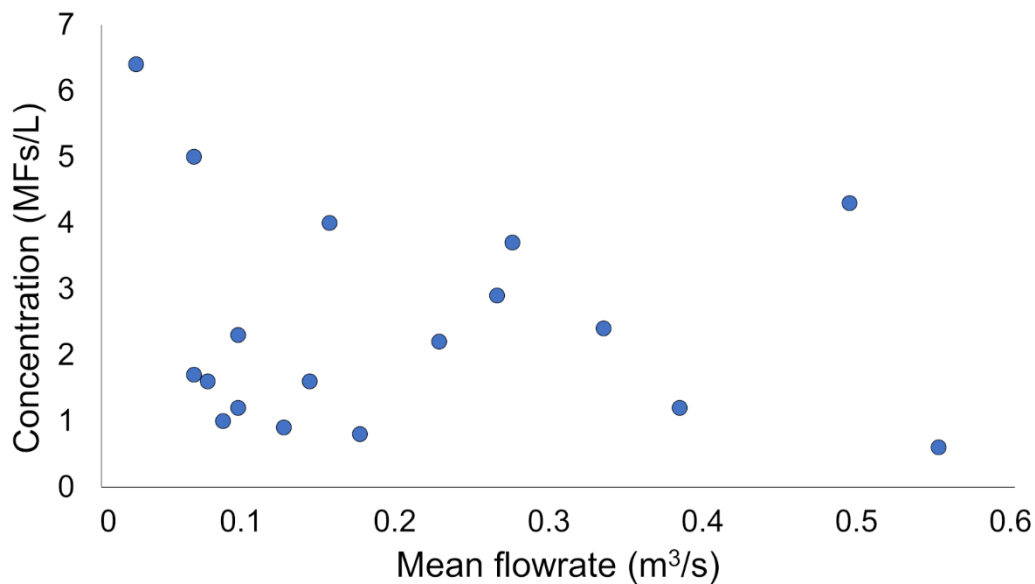
472 polyvinyl chloride; PA: polyamide; PS: polystyrene.

473

474 Table S1: Sampling volumes and number of fibers counted for each sample

	Volume (L)	Number of fibers counted
June 2018-1	103.5	467
June 2018-2	103.05	322
June 2018-3	102.6	431
June 2018-4	104.9	150
June 2018-5	101.2	192
December 2018-1	82.1	331
December 2018-2	84.8	75
December 2018-3	87.1	235
December 2018-4	87.1	169
December 2018-5	86.2	171
March 2019-1	102.6	122
March 2019-2	83.9	219
March 2019-3	86.2	131
March 2019-4	86.7	93
March 2019-5	87.6	113
May 2019-1	83	211
May 2019-2	85.3	452
May 2019-3-10%	88	59

475



476

477 Figure S6: Concentration of microfibers (MFs) in items/L versus the mean flow rate (m³/s) of

478 each sampling period.